Opening space for H_2 storage: Cointercalation of graphite with lithium and small organic molecules

Yufeng Zhao,* Yong-Hyun Kim, Lin J. Simpson, Anne C. Dillon, Su-Huai Wei, and Michael J. Heben
National Renewable Energy Laboratory, Golden, Colorado 80401, USA
(Received 22 July 2008; published 6 October 2008)

Cointercalation of graphite with lithium and organic molecules, such as benzene and tetrahydrofuran (THF), is studied using first-principles calculations. The molecules play an important role in expanding the interlayer graphene distance to ~7.7 Å. The increased space permits multiple H_2 species to be bound to Li cations with a binding energy of 10–22 kJ/mol. Furthermore, in the interstitial area free of Li cations, the negative charge in the graphene sheets enhances the H_2 binding energy to ~9 kJ/mol through electrostatic attraction. In order to restrain nucleation of lithium hydrides, the densest Li array is determined to be a $Li_4(THF)C_{72}$ structure, which absorbs 3.4 wt % hydrogen molecules reversibly. Cointercalation offers an experimentally accessible approach to designing optimized hydrogen storage materials that have not been investigated previously.

DOI: 10.1103/PhysRevB.78.144102 PACS number(s): 61.66.Hq, 71.20.Tx, 81.05.Uw

The idea of using coordinately unsaturated metal centers supported on carbon frameworks[1,2] for construction of high-capacity ambient-temperature reversible hydrogen sorption materials has prompted many new theoretical designs[3–7] and experimental efforts.[8–13] A central challenge in realizing the benefits of the approach is to simultaneously maintain open free space while keeping active metal centers dispersed on a highly durable material. The latest theoretical investigations have focused on achieving metal dispersion using materials with intrinsic porosity, e.g., metal organic frameworks (MOF),[14,15] or exfoliated graphitic materials.[6,16–19] The ability of MOFs to be stable with intense functionalization is a concern, while large surface-area materials which are expected to be more stable, such as zeolite-templated carbons,[20] have pores which may be too large. As for graphitic materials, current efforts are still limited to hypothetical structures[6,16,19] or artificial spacing.[17,18]

Although it is attractive to consider opening space for physisorption in graphite, which is a cheap and durable material, it is not clear how the relatively large spacing that have been named "ideal" may be practically achieved. The idea of using C_{60}-intercalated graphite for hydrogen storage is stimulating,[16,21] but C_{60} molecules inherently create a large fraction of inaccessible space inside the material, which diminishes the hydrogen capacity. It is well known that graphite can be intercalated with alkaline or alkaline-earth metals to form compounds in which the metal atoms are ionized by the electronegative graphene sheets. H_2 molecules can be absorbed by such materials at a temperature below 200 K,[22,23] but the capacity is too low for practical application because there is no sufficient open space. Also, the high metal density makes the compound highly reducing such that H_2 molecules are dissociated to form hydride above 200 K.[23] To increase molecular H_2 sorption, the graphitic planes must be further opened and the metal concentration should be lowered. Fortunately, some small molecules, e.g., N_2,[24] NH_3,[25] benzene, and tetrahydrofuran (THF),[26] can be absorbed into metal-intercalated graphite to expand the interlayer graphene distance from 4–5 to 7–9 Å.[26] To our best knowledge, there is no report on hydrogen storage in such cointercalated graphite. This area may offer many advantageous possibilities in material sciences.

In this paper, we show that a proper balance of competing considerations can lead to the formation of remarkable hydrogen storage materials through cointercalation processes. The balance is achieved through the selection of the right metal species, the right molecular species, and the optimum metal density. Here we focus on Li metal because of its light weight and the fact that Li exhibits the best binding energy with H_2 among all alkaline metals,[27] whereas nonalkaline metals (e.g., alkaline-earth or transition metals) are extremely difficult to fully disperse. Among all potentially intercalating molecules, including N_2, NH_3, and C_{60}, we focus on THF and benzene because they can expand the interlayer distance ideally while being low weight. To maximize the hydrogen capacity, we determine the maximum metal density at which the Li cations remain homogeneously dispersed throughout the whole material system.

We use the first-principles density-functional theory (DFT) method implemented in the Vienna *Ab initio* Simulation Package.[28] A plane-wave basis set (500 eV cutoff) is used in combination with an all-electron-like projector augmented-wave potential and Perdew-Burke-Ernserhof exchange-correlation functional within the generalized gradient approximation.[29] Three-dimensional (3D) periodic condition is applied to the unit cell with a two-dimensional (2D) graphene supercell in the x-y plane and the interlayer distance in z direction optimized. The structures are considered to be in equilibrium when the force acting on the atoms drops below 0.005 eV/Å.

Employing a 4×6 graphene supercell as the computing unit cell, we first simulate the basic properties of a $Li_2(THF)C_{48}$ structure interacting with hydrogen molecules. Each unit cell contains one graphene layer, one THF (or benzene) molecule, and two Li atoms. Hexagonal 6×6 supercells are then used to study a series of structures, $Li_x(THF)C_{72}$, with metal density being varied following $x=2$, 4, 6, and 8. To sample the Brillouin zone, the Monkhorst-Pack-type meshes are generated automatically with the sizes of $2\times2\times4$ for the 4×6 supercells and $1\times1\times4$ for the 6×6 supercells. The lattice constant for the 2D graphene sheet is optimized to be 2.468 Å. Although the DFT method is well known for its inability in dealing with

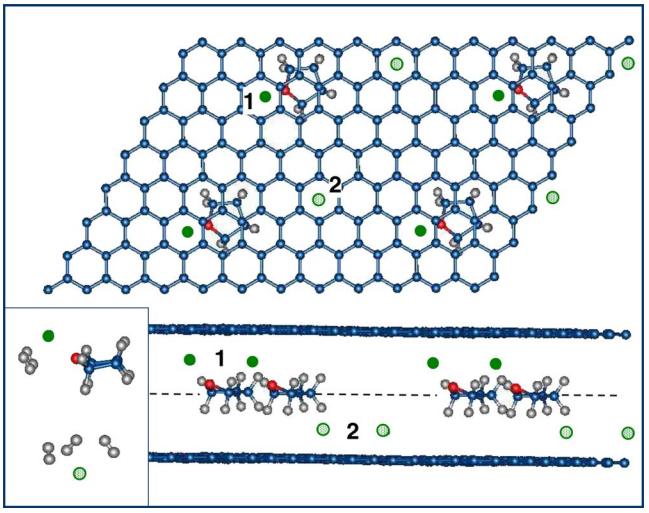

FIG. 1. (Color online) Top and side views of the crystal structure of $Li_2(THF)C_{48}$. Carbon, hydrogen, oxygen, and lithium atoms are denoted, respectively, by blue, gray, red, and green balls. The upper Li atoms (solid green balls closer to the top graphene sheet) are attached to the oxygen atoms in the THFs, and the lower Li atoms (shaded green balls closer to the bottom sheet) are away from the THFs. Inset: each Li-1 site (Li-2 site) can bind two (three) dihydrogen molecules in side views.

the van der Waals (vdW) interaction, the calculated binding energy of H_2 to a graphene sheet, 5.8 kJ/mol H_2, happens to agree well with experimental value of 4–5 kJ/mol H_2. Because this study is focused on binding enhancement due to electrostatic interaction, the DFT error for vdW will not affect our conclusion.

First, we discuss the structures of $Li_2(THF)C_{48}$ and $Li_2(C_6H_6)C_{48}$ and their interactions with hydrogen. When THF molecules are incorporated in Li-intercalated graphite, the interlayer distance of graphite is substantially increased. Therefore, the Li atoms originally sandwiched in the middle plane between two neighboring graphene layers (dashed line in Fig. 1) are now moved into two separate planes in an alternating fashion (solid/shaded green balls in Fig. 1), and the Li-Li distance is increased. The Li atoms interact with the cointercalating organic molecules before H_2 molecules are incorporated. In the unit cell of $Li_2(THF)C_{48}$, one Li (denoted as Li-1) is close to the O atom in the THF, and the other one (Li-2) is located roughly in the center of three neighboring THFs (Fig. 1). The Li-1 atoms are bound very strongly (2.81 eV/atom) between the graphene and the THF molecules, and the binding energy of Li-2 atoms to the graphene sheet is 1.91 eV/atom. The interlayer graphene distance is 7.73 Å, which is much larger than that of 3.94 Å in LiC_{24} but very close to the optimal value at which remarkable properties of physisorption of H_2 have been predicted.[18] Because more space is opened, each Li cation can interact only with one graphene sheet and is therefore available to bind H_2 molecules. Our calculation shows that Li-1 binds two H_2 molecules with the binding energy of 10–12 kJ/mol, and that each Li-2 cation binds three dihydrogen molecules with binding energies of 11–22 kJ/mol (see Table I). The average binding energy of 13.9 kJ/mol is close to the optimal value of 15 kJ/mol for ambient reversible hydrogen storage.[30] Note that the binding energies calculated here for the three H_2 molecules bound to Li-2 sites agree well with calculations for Li-decorated MOF.[14] The mechanism of Li^+-H_2 interaction is interpreted in terms of electrostatic charge-quadrupole and charge-induced dipole forces,[27,31] which lead to stronger H_2 binding when a small cation such as Li^+ rather than Na^+ and K^+ is employed.

TABLE I. Binding energy (kJ mol^{-1})/H-H bond length (Å) of H_2 bound to the two Li sites in $Li_2(THF)C_{48}$. Li-1 is the Li atom attached to the THF, and Li-2 is the isolated one on the graphene sheet (Fig. 1). The H-H bond length of a free H_2 molecule is 0.750 Å in this calculation.

	Li-1	Li-2
1	12.6/0.755	22.6/0.756
2	10.1/0.755	18.8/0.756
3		11.8/0.755

If the THFs are replaced with benzene molecules, the two Li cations in the unit cell are attracted to the benzene ring and form a double sandwiched structure with the benzene and two graphene sheets (Fig. 2). Simulation indicates that these Li atoms no longer bind H_2. However, with an interlayer distance of 7.68 Å, benzene cointercalation still opens space for physisorption.

In principle, at low metal density when no metal-metal bonds are formed, the total hydrogen capacity increases linearly with the metal density.[32] However, as the metal density increases, the degree of metal ionization will be lowered and metal-metal attraction eventually emerges. This reduces hydrogen uptake either by metal clustering[33] or more seriously by forming the metal hydride phase.[8] To find the maximum capacity, the maximum nonclustering Li density must be determined. For this purpose, a superstructure, $Li_x(THF)C_{72}$ in a 6×6 graphite unit cell, was constructed with one THF molecule and an increasing number of Li atoms ($x=2$, 4, 6, 8, and 10) and the total energies for both the Li-dispersed and Li-clustering structures were calculated. For full dispersion, the Li-Li distance is geometrically maximized (see Fig. 3) in every input structure, which is subsequently computationally relaxed. The Li atoms are found to form clusters spontaneously at $x=10$. From this $Li_{10}(THF)C_{72}$ structure, the Li-clustered structures for $x=8$, 6, and 4 were generated by removing two Li atoms in each step and relaxed again. The increasing Li-Li distance in the clustered structures in-

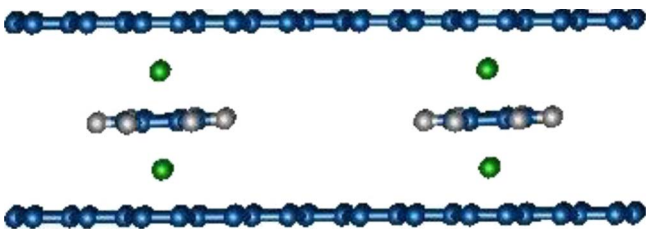

FIG. 2. (Color online) Side view of crystal structure of $Li_2(C_6H_6)C_{48}$. The interlayer graphene distance is 7.68 Å but the Li cations cannot bind dihydrogen.

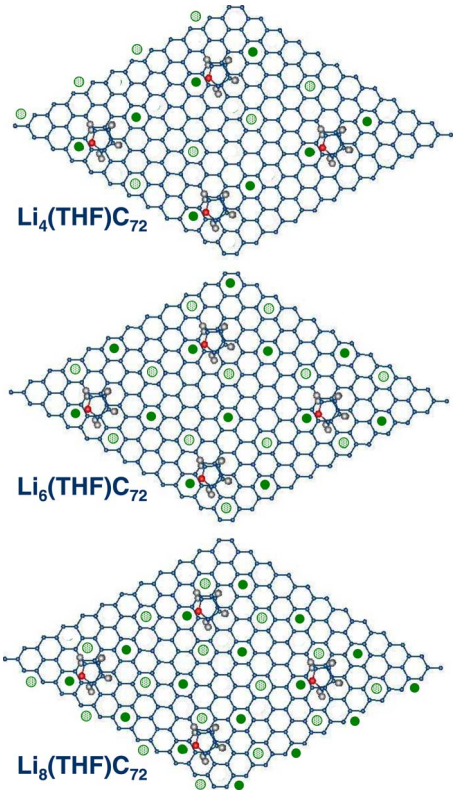

FIG. 3. (Color online) Top views of the Li-dispersed $Li_x(THF)C_{72}$ structures (x=4, 6, and 8). The upper and lower Li atoms are again denoted by solid and shaded green balls.

dicates a tendency of Li-cluster dissociation as the number of Li atoms decreases. This is clearly shown in Table II: the nearest-neighbor Li-Li distance gradually increases from 2.8 to 5.2 Å with x decreasing from 8 to 4, and the total energy of the clustered structure relative to the dispersed ones goes up. Eventually, the "clustered" structure becomes energetically less favorable than the fully dispersed one at x=4. We found that the fully dispersed $Li_4(THF)C_{72}$ structures have the widest electronic band gap with a Fermi level 0.4 (1.2) eV lower than the Li-clustered (Li-dispersed) $Li_6(THF)C_{72}$. This can be explained by the semimetal electronic structure of graphite, which opens a gap of 1.5 eV upon intercalation with THFs, due to the break of symmetry. When four Li atoms are incorporated, the Li electrons fill the valence band completely without occupying the conduction bands. This renders the $Li_4(THF)C_{72}$ a wide-gap salt and is critically important for preventing H_2 from dissociating into hydrides because the electron donation to H_2 will be significantly restrained. In contrast, H_2 molecules may be dissociated effectively in the metallic $Li_6(THF)C_{72}$ structure, which has a similar in-plane metal density as the stage-two compound MC_{24}. Therefore the maximum Li density for molecular hydrogen storage should be as low as in $Li_4(THF)C_{72}$. This calls for a rethinking of high Li density decoration of carbon-based frameworks.[15,17,34]

TABLE II. Total energy (eV)/electronic band gap (eV)/nearest-neighboring Li-Li distance (Å) of $Li_x(THF)C_{72}$ structures (x=4, 6, and 8) with clustered and fully dispersed Li arrays.

	$Li_4(THF)C_{72}$	$Li_6(THF)C_{72}$	$Li_8(THF)C_{72}$
Clustered	0.37/0.89/5.2	−0.94/0.72/3.2	−2.45/0.77/2.8
Dispersed	0/1.29/7.4	0/0.14/6.1	0/0.05/5.7

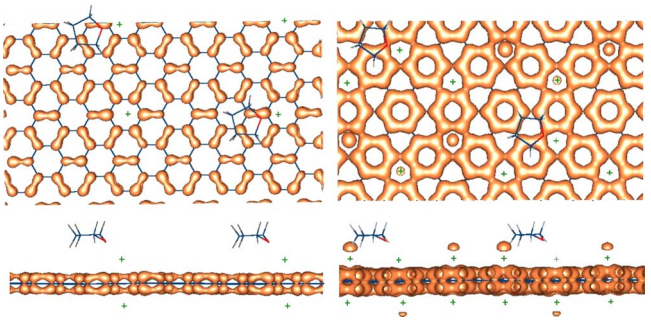

FIG. 4. (Color online) Charge density of the two/six electrons in the highest occupied bands of $Li_2(THF)C_{72}$(left)/$Li_6(THF)C_{72}$ (right). Top (upper panels) and side views (lower panels) are shown. The honeycomb patterns are around the graphene sheets, and the mushroom-shaped patterns are localized on top of Li cations. All the electrons occupying the lower eigenstates (not shown here) are localized around the graphene sheet.

Table II indicates that Li clustering (bonding) overcomes Coulomb repulsion as charge transfer to the graphene sheets per Li atoms decreases (i.e., residual charge in Li increases) at higher Li density (see Fig. 4). As a general rule for design of metal-based hydrogen sorbents, enhancing charge transfer to overcome metal-metal bonding is the key to effective metal dispersion.[1,32] Consequently, it is expected that the metal atoms with higher electronegativity and valence are much more difficult to disperse. As examples, we simulated the structures of $Ca_2(THF)C_{36}$ and $Ca_2(THF)C_{48}$, observing that the two Ca atoms in the unit cell spontaneously form a dimer. In this case hydrides always form due to electron donation from the metal bonds to H_2. All these results indicate the favorability of the low Li density as in $Li_4(THF)C_{72}$.

The $Li_4(THF)C_{72}$ structure interacts with hydrogen (see Table III and Fig. 5) in a similar way to $Li_2(THF)C_{48}$. The Li-1 cation attached to the THF oxygen binds two H_2 molecules and each of the three Li-2 cations binds three. In addition to these eleven H_2 molecules bound to the Li atoms, six more H_2 molecules in each unit cell are adsorbed in the interstitial sites as marked by the dashed circles in Fig. 5. The H-H bonds of these "floating" H_2 are perpendicular to

TABLE III. Hydrogen binding energy (kJ/mol) of the two types of Li sites in $Li_4(THF)C_{72}$. The underlined value in the right most column is the average binding energy of six hydrogen molecules adsorbed in the interstitial sites.

	Li-1	Li-2	
1	12.6	22.4	
2	9.3	17.6	
3		13.6	
			9.1

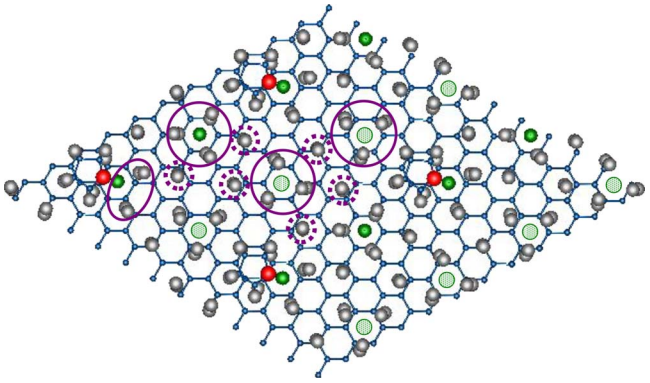

FIG. 5. (Color online) Top views of the $(H_2)_{17}Li_4(THF)C_{72}$ structure. The H_2 molecules bound closely to Li are marked by solid circles while those in the interstitial sites by dashed circles.

the graphene plane. Such geometry enhances H_2 binding (9.1 kJ/mol in Table III) over that of a single graphene sheet (5.8 kJ/mol). The calculated binding energy of 9.1 kJ/mol is comparable to the value measured for H_2 sorption in MC_{24} (M =K, Rb, and Cs).[23] To examine the origin of this enhancement, we calculated the pure vdW binding of H_2 molecules between two graphene sheets artificially spaced by 7.73 Å (without Li) and obtained a binding energy of 7.3 kJ/mol. Therefore, the two-side contact enhances H_2 binding only by 1.5 kJ/mol, while the extra 1.8 kJ/mol enhancement is due to the electrostatic attraction between the positive ends of H_2 polar potential[31] and the negatively charged graphene sheets upon Li intercalation. The total hydrogen capacity in this structure is 3.4 wt %, which is slightly higher than the Li-decorated MOF (Ref. 14) and the Li-doped carbon nanoscrolls with an artificially separated intershell distance of 8 Å.[17]

Finally, we include a brief discussion of the approaches to synthesis. The energy gain per THF molecule for the energetically favorable reaction $LiC_{72}+THF \rightarrow Li(THF)C_{72}$ is 0.32 eV. However, for the reaction $Li_2C_{72}+THF \rightarrow Li_2(THF)C_{72}$, there is an energy cost of 0.21 eV per THF. Generally, for a fixed y in $Li_x(THF)C_y$, the larger the x, the less favorable the reaction $Li_xC_y+THF \rightarrow Li_x(THF)C_y$ because Li_xC_y is a very stable compound. This means that it is difficult to synthesize $Li_x(THF)C_y$ directly from Li_xC_y when $x>1$. To circumvent such a difficulty, we propose a two-step reaction as follows:

$$LiC_y + THF \rightarrow Li(THF)C_y,$$

$$Li(THF)C_y + Li_{x-1} \rightarrow Li_x(THF)C_y.$$

The first step is energetically favorable. The second step can always be realized by raising the chemical potential of Li_{x-1}, for example, in a vaporized Li atom reservoir.

Although we arbitrarily chose THF density in this study, high hydrogen capacity requires a low THF density and therefore a low Li density in the first step. Experimental control of the THF density should be studied. Also, it should be pointed out that water is harmful for the Li cations and should be avoided in the synthetic process.[35]

In summary, a practical pathway to hydrogen storage in adsorptive materials functionalized with active metal centers is proposed by cointercalating graphite with metal and small molecules. The metal atoms initiate the intercalation while the cointercalating species open more free space. Lithium is the best metal due to its light weight, low electronegativity, and strong electrostatic interaction with H_2. The THF molecule is identified as a good cointercalant since it binds only one Li atom and still leaves room for this Li atom to bind H_2 molecules. Charge transfer from metal to graphene sheets plays a triple role: it ionizes and stabilizes the dispersed metal arrays, it enhances the H_2 binding to the metal center, and it enhances the H_2 binding directly to the graphene sheets. Our study opens a different area of research for the design of hydrogen sorbents. Also, we show that the density of Li atoms must be surprisingly low to prevent agglomeration and formation of metal hydrides.

This work was supported by the Office of Science, Basic Energy Sciences, Division of Materials Science, the Office of Energy Efficiency and Renewable Energy Hydrogen, Fuel Cell, and Infrastructure Technologies Program of the U.S. Department of Energy through the Hydrogen Sorption Center of Excellence under Grant No. DE-AC36-99GO10337. Computing time was provided by DOE's National Energy Research Scientific Computing Center.

*Corresponding author; yufend_zhao@nrel.gov

[1] Y. Zhao, Y. H. Kim, A. C. Dillon, M. J. Heben, and S. B. Zhang, Phys. Rev. Lett. **94**, 155504 (2005).
[2] T. Yildirim and S. Ciraci, Phys. Rev. Lett. **94**, 175501 (2005).
[3] H. Lee, W. H. Choi, and J. Ihm, J. Alloys Compd. **446-447**, 373 (2007).
[4] H. Lee, W. I. Choi, and J. Ihm, Phys. Rev. Lett. **97**, 056104 (2006).
[5] S. Meng, E. Kaxiras, and Z. Zhang, Nano Lett. **7**, 663 (2007).
[6] N. Park *et al.*, J. Am. Chem. Soc. **129**, 8999 (2007).
[7] Y. Zhao *et al.*, Chem. Phys. Lett. **425**, 273 (2006).
[8] A. C. Dillon *et al.*, Phys. Status Solidi B **244**, 4319 (2007).
[9] X. Hu, M. Trudeau, and D. M. Antonelli, Chem. Mater. **19**, 1388 (2007).
[10] P. Jain *et al.*, J. Phys. Chem. C **111**, 1788 (2007).
[11] S. Rather *et al.*, Chem. Phys. Lett. **441**, 261 (2007).
[12] X. L. Wang and J. P. Tu, Appl. Phys. Lett. **89**, 064101 (2006).
[13] A. B. Phillips and B. S. Shivaram, Phys. Rev. Lett. **100**, 105505 (2008).
[14] A. Blomqvist *et al.*, Proc. Natl. Acad. Sci. U.S.A. **104**, 20173 (2007).
[15] S. S. Han and W. A. Goddard, J. Am. Chem. Soc. **129**, 8422 (2007).
[16] A. Kuc *et al.*, Nano Lett. **7**, 1 (2007).

[17] G. Mpourmpakis, E. Tylianakis, and G. E. Froudakis, Nano Lett. **7**, 1893 (2007).
[18] S. Patchkovskii *et al.*, Proc. Natl. Acad. Sci. U.S.A. **102**, 10439 (2005).
[19] W. Q. Deng, X. Xu, and W. A. Goddard, Phys. Rev. Lett. **92**, 166103 (2004).
[20] Z. Yang, Y. Xia, and R. Mokaya, J. Am. Chem. Soc. **129**, 1673 (2007).
[21] V. Gupta *et al.*, Solid State Commun. **131**, 153 (2004).
[22] N. Akuzawa *et al.*, Synth. Met. **34**, 701 (1990).
[23] T. Enoki *et al.*, J. Mater. Res. **5**, 435 (1990).
[24] R. Moreh, S. Melloul, and H. Zabel, Phys. Rev. B **47**, 10754 (1993).
[25] J. M. Zhang, P. C. Eklund, Y. B. Fan, and S. A. Solin, Phys. Rev. B **38**, 10878 (1988).
[26] A. Charlier, R. Setton, and M. F. Charlier, Phys. Rev. B **55**, 15537 (1997).
[27] R. C. Lochan and M. Head-Gordon, Phys. Chem. Chem. Phys. **8**, 1357 (2006).
[28] G. Kresse and J. Furthmuller, Phys. Rev. B **54**, 11169 (1996).
[29] J. P. Perdew, K. Burke, and M. Ernzerhof, Phys. Rev. Lett. **77**, 3865 (1996).
[30] S. K. Bhatia and A. L. Myers, Langmuir **22**, 1688 (2006).
[31] G. J. Vitillo *et al.*, J. Chem. Phys. **122**, 114311 (2005).
[32] Y. Zhao *et al.*, Nano Lett. **8**, 157 (2008).
[33] O. Sun *et al.*, J. Am. Chem. Soc. **127**, 14582 (2005).
[34] Q. Sun *et al.*, J. Am. Chem. Soc. **128**, 9741 (2006).
[35] R. T. Yang, Carbon **38**, 623 (2000).